




# Cx43 regulates mechanotransduction mechanisms in human preterm amniotic membrane defects

Eleni Costa<sup>1</sup> | Christopher Thrasivoulou<sup>2</sup> | David L. Becker<sup>3</sup> | Jan A. Deprest<sup>4,5</sup>  | Anna L. David<sup>4,5</sup>  | Tina T. Chowdhury<sup>1</sup> 

<sup>1</sup>Centre for Bioengineering, School of Engineering and Materials Science, Queen Mary University of London, London, UK

<sup>2</sup>Department of Cell and Developmental Biology, University College London, London, UK

<sup>3</sup>Lee Kong Chian School of Medicine, Nanyang Technological University, Singapore, Singapore

<sup>4</sup>Department of Obstetrics and Gynaecology, University Hospitals Leuven, Leuven, Belgium

<sup>5</sup>Elizabeth Garrett Anderson Institute for Women's Health, University College London, Medical School Building, London, UK

## Correspondence

Tina T. Chowdhury, Centre for Bioengineering, School of Engineering and Materials Science, Queen Mary University of London, Mile End Road, London E1 4NS, UK.  
Email: [t.t.chowdhury@qmul.ac.uk](mailto:t.t.chowdhury@qmul.ac.uk)

## Funding information

Great Ormond Street Hospital for Children, Grant/Award Number: 17QMU01; Rosetrees Trust, Grant/Award Number: M808

## Abstract

**Objective:** The effects of mechanical stimulation in preterm amniotic membrane (AM) defects were explored.

**Methods:** Preterm AM was collected from women undergoing planned preterm caesarean section (CS) due to fetal growth restriction or emergency CS after spontaneous preterm prelabour rupture of the membranes (sPPROM). AM explants near the cervix or placenta were subjected to trauma and/or mechanical stimulation with the Cx43 antisense. Markers for nuclear morphology (DAPI), myofibroblasts ( $\alpha$ SMA), migration (Cx43), inflammation (PGE<sub>2</sub>) and repair (collagen, elastin and transforming growth factor  $\beta$  [TGF $\beta$ <sub>1</sub>]) were examined by confocal microscopy, second harmonic generation, qPCR and biochemical assays.

**Results:** In preterm AM defects, myofibroblast nuclei were highly deformed and contractile and expressed  $\alpha$ SMA and Cx43. Mechanical stimulation increased collagen fibre polarisation and the effects on matrix markers were dependent on tissue region, disease state, gestational age and the number of fetuses. PGE<sub>2</sub> levels were broadly similar but reduced after co-treatment with Cx43 antisense in late sPPROM AM defects. TGF $\beta$ <sub>1</sub> and Cx43 gene expression were significantly increased after trauma and mechanical stimulation but this response dependent on gestational age.

**Conclusion:** Mechanical stimulation affects Cx43 signalling and cell/collagen mechanics in preterm AM defects. Establishing how Cx43 regulates mechanosignalling could be an approach to repair tissue integrity after trauma.

## Key points

### What's already known about this topic?

- In term amniotic membrane (AM), mechanical stimulation increased Cx43 plaque formation that prevents migration and healing by amniotic mesenchymal cells (AMCs).
- Cx43 also increased myofibroblast migration to the wound edge, resulting in cell/collagen contraction, healing and closure of the defect site.

Oral presentation LC-11 <https://obgyn.onlinelibrary.wiley.com/doi/10.1002/pd.6283> Eleni Costa, Chris Thrasivoulou, Jan Deprest, David Becker, Anna David, Tina Chowdhury. Mechanotransduction mechanisms in human preterm fetal membranes after trauma and Cx43 knockdown. 26th ISPD, Montréal, Canada, 20–22 June 2022.

This is an open access article under the terms of the [Creative Commons Attribution-NonCommercial](https://creativecommons.org/licenses/by-nc/4.0/) License, which permits use, distribution and reproduction in any medium, provided the original work is properly cited and is not used for commercial purposes.

© 2023 The Authors. Prenatal Diagnosis published by John Wiley & Sons Ltd.

**What does this study add?**

- In preterm AM defects, mechanical stimulation increased cell deformation in the fibroblast layer and collagen polarisation around the wound edge.
- Mechanical stimulation increased Cx43 in myofibroblasts and amniotic epithelial cells, but this response was dependent on tissue region.
- Markers for migration, inflammation and repair were influenced by mechanical stimulation.

**1 | INTRODUCTION**

Fetal membranes are essential for immune and mechanical protection of the fetus and the delivery of a healthy baby after term rupture and labour. The mechanisms underlying scheduled rupture as the pregnancy approaches term are complex, regulated by mechanical forces with advancing gestation.<sup>1–4</sup> It is known that Infection, wounds created after iatrogenic surgery and uterine overdistention increase inflammatory, prostaglandin and protease factors that degrade structural proteins like collagen in the amniotic membrane (AM) leading to spontaneous preterm prelabour rupture of the fetal membranes (sPPROM).<sup>4–11</sup> There are few reports that demonstrate how mechanical stimulation before 30 weeks of gestation regulates mechanotransduction in preterm AM. A deeper understanding of the mechanisms will help to identify targets that promote collagen structural integrity to term and aid prevention or improve the management of PPRM.<sup>12,13</sup>

Several *in vitro* term models investigated the effects of mechanical stimulation on cell behaviour using human monolayer conditions or 3D tissue explants subjected to stretch or organ-on-chip systems.<sup>14–23</sup> In monolayer culture, static stretch (11%) of Amniotic Epithelial Cells (AECs) increased nuclear factor-kappaB (NF- $\kappa$ B) activation of cyclooxygenase-2 (COX-2) expression and prostaglandin E<sub>2</sub> (PGE<sub>2</sub>) release.<sup>16,19</sup> In AM explants, cyclic stretch increased other NF $\kappa$ B regulated genes such as interleukin-1 $\beta$  (IL-1 $\beta$ ), interleukin-6 (IL-6) and interleukin-8 (IL-8), tumour necrosis factor  $\alpha$  (TNF $\alpha$ ) or matrix metalloproteinase (MMP) enzymes.<sup>24–26</sup> After stretch, increased secretion of cytokines enhanced apoptotic pathways by AECs and amniotic mesenchymal cells (AMCs), which degrade collagen and reduced tensile strength in the fibroblast layer and basement membrane of AM.<sup>2,4,9,20,27–30</sup> In organ-on-chip system cultured with five cell types from term fetal membranes and decidua, treatment with lipopolysaccharide (LPS) differentially increased cytokines and TNF $\alpha$  by cells from the chorionic membrane (CM) and induced repair mechanisms in the AM.<sup>31</sup> The epithelial to mesenchymal transition (EMT) mechanism was enhanced by differentiation of AEC to AMC phenotype in response to trauma, hydrostatic pressure or inflammation.<sup>2,8,9,28,29,31,32</sup> Whilst mechanical stimulation in the form of cyclic stretch or shear in organ-on-chip systems has yet to be identified in preterm cells, the 3D model demonstrates that cell type plays an important role when dissecting the inflammatory cascade by pathway manipulation strategies. In term AM, we and others have shown that mechanical stimulation affects collagen organisation, synthesis, degradation and tissue strength.<sup>5,6,12,21,27,33,34</sup> In term AM, mechanical stimulation differentially upregulates the gap junction protein connexin 43 (Cx43) and

forms plaques between AMCs preventing cell migration and repair.<sup>35</sup> In contrast, the highly contractile myofibroblasts expressed Cx43 localised in the cytoplasmic processes and promote repair via  $\alpha$ -smooth muscle actin ( $\alpha$ SMA) and release of transforming growth factor sub-type 1 (TGF $\beta$ <sub>1</sub>).<sup>36</sup> Depending on the localisation and concentration of Cx43, this mechanoreceptor therefore mediates multiple functions such as differentiation, migration, healing and inflammation in term AM wounds.<sup>35–39</sup> In preterm AM defects, we hypothesised that mechanical stimulation activates a Cx43-stretch sensitive pathway and increases healing by myofibroblasts and cell/collagen contraction. We examined the effects of mechanical stimulation on Cx43 expression and collagen organisation in preterm AM and explored whether Cx43 knockdown could affect wound healing signals and tissue integrity.

**2 | METHODS****2.1 | Research ethics and sample collection**

Human placentas ( $n = 13$ ) were collected after elective or emergency caesarean section with written informed consent from women who delivered at University College London (UCL) Hospital (UCLH). Ethical approval was granted by the Joint UCL and UCLH committees, the National Research Ethics Service Committee London, Bloomsbury and the Ethics of Human Research Central Office (Reference 14/LO/0863). All methods were performed according to the relevant guidelines and regulations of UCL, UCLH and Queen Mary University of London (QMUL).

**2.2 | Clinical diagnosis**

Information on included patients with spontaneous PPRM is presented in Table 1. The patients were classified into the following two groups using clinical diagnosis: Group 1: Iatrogenic preterm birth due to fetal growth restriction (FGR) and/or pre-eclampsia with singleton ( $n = 5$ ) or twin pregnancies ( $n = 3$ ) and Group 2: early sPPROM from 27 to 31 weeks gestation ( $n = 2$ ) or late sPPROM  $\geq 32$ -week gestation ( $n = 3$ ). In the early sPPROM group, one patient had suspected clinical chorioamnionitis within 24 h after delivery and in the late sPPROM group, one patient had bleeding due to fibroids and placenta previa (Table 1). We did not include women who experienced a prolonged latency period greater than 48 h after the onset of early or late sPPROM due to the high risk of chorioamnionitis.

TABLE 1 Clinical diagnosis of included cases with spontaneous PPROM.

Case	Maternal age (years)	GA at delivery (weeks + days)	Clinical diagnosis	Obstetric complications	Singleton or twin gestation
1	34	35 + 5	Iatrogenic PTB	FGR	Singleton
2	39	35 + 6	Iatrogenic PTB	FGR	Singleton
3	38	34 + 0	Iatrogenic PTB	FGR	Singleton
4	30	29 + 0	Iatrogenic PTB	FGR	Singleton
5	31	33 + 0	Iatrogenic PTB	FGR and teratoma	Singleton
6	40	33 + 0	Iatrogenic PTB	FGR	Twin DCDA
7	32	34 + 6	Iatrogenic PTB	FGR	Twin MCMA
8	42	33 + 0	Iatrogenic PTB	FGR with stillbirth of one twin at 30 + 0	Twin DCDA
9	32	27 + 0	sPPROM $\leq$ 32 weeks	Vaginal bleeding	Singleton
10	27	29 + 1	sPPROM $\leq$ 32 weeks	Emergency CS due to abnormal CTG. Defect size $\sim 1.5 \times 2$ cm	Singleton
11	32	35 + 6	sPPROM $\geq$ 32 weeks	Placental insufficiency defect size $\sim 2.5 \times 3$ cm	Singleton
12	39	35 + 5	sPPROM $\geq$ 32 weeks	Placental insufficiency	Singleton
13	30	33 + 6	sPPROM $\geq$ 32 weeks	Placenta previa, bleeding and fibroids	Singleton

Note: All patients delivered preterm before 37 + 0 weeks GA. For all experimental investigations, patients were grouped into three classifications by clinical diagnosis namely FGR for singleton ( $n = 5$ ) or twin ( $n = 3$ ) deliveries, sPPROM  $\leq$ 32 weeks ( $n = 2$ ) and  $\geq$ 32 weeks ( $n = 3$ ). All deliveries were performed by either scheduled or emergency CS.

Abbreviations: CS, caesarean-section; FGR, fetal growth restriction; GA, gestational age; sPPROM, spontaneous preterm prelabour rupture of the membranes.

### 2.3 | Amniotic membrane tissue isolation

At Caesarean section after delivery of the baby but before delivery of the placenta, a sterile clip was placed on the lower edge of the tissue within the uterine incision to provide a landmark. The placenta was separated from the uterus by gentle cord traction and rinsed with Earle's Balanced Salt Solution (EBSS) for 3 min to remove excess maternal blood (Sigma-Aldrich). AM was separated from the CM and placenta using gentle traction. The orientation of the membrane to the placenta, incision line and cervix was noted throughout the procedure and the AM nearest the cervix was identified using a clip. Dumbbell shaped AM specimens measuring widths in the gauge and shoulder regions of  $10 \times 25$  mm were dissected from the cervix (CAM) and placenta (PAM) regions and equilibrated 1 mL of Dulbecco's modified Eagle's medium (DMEM) supplemented with 5  $\mu$ g/ml penicillin, 5  $\mu$ g/ml streptomycin, 15  $\mu$ g/ml ascorbate and 20% Fetal Calf Serum (FCS) prior to mechanical loading experiments.

### 2.4 | Mechanical loading

Human CAM and PAM specimens were secured within a BOSE loading frame (BOSE Corporation) at 37°C. Serum-free media was supplemented with 0 or 50  $\mu$ M Cx43 antisense (inhibits Cx43 mRNA expression). Strained AM specimens were subjected to 2% cyclic tensile strain (CTS) at 1 Hz frequency applied intermittently (1 min CTS followed by 9 min unstrained) for 24 h, as described.<sup>21,35</sup> In separate experiments, a 0.8 mm defect was created with a 21G

needle in the explant to mimic trauma and subjected to CTS. In control experiments, specimens were taken from the same donor and cultured without mechanical stimulation (–CTS).

### 2.5 | Tissue preparation for immunostaining

AM specimens were fixed in 4% PFA for 2 h and incubated together with primary antibodies for mouse Cx43 (1:100, ThermoFisher Scientific, CX-1B1) and rabbit  $\alpha$ SMA (1:100, Abcam, ab5694) at 4°C overnight, as described.<sup>36</sup> Specimens were washed in PBS and incubated with secondary antibodies for Alexa Fluor 568 anti-mouse or 488 anti-rabbit at room temperature for 2 h (both 1:1000, ThermoFisher Scientific) and counterstained with 1  $\mu$ g/mL DAPI for 20 min (1:1000) to detect nuclei. Secondary antibody incubation in the absence of the primary antibody was used as a negative control.

### 2.6 | Second harmonic generation and confocal imaging

Specimens were imaged by two-photon confocal imaging on a Leica TCS SP8 acousto-optic beam splitter multiphoton confocal laser scanning microscope (Leica) with a Coherent Chameleon Ultra, Ti Sapphire mode locked IR laser (Coherent UK Ltd). Samples were imaged at excitation/emission wavelengths of 405/460 nm for DAPI, 495/518 nm for  $\alpha$ SMA and 578/603 nm for Cx43 as previously described.<sup>35,36</sup> A transmission detector was used for the collection of

collagen SHG signal with a 430–450 nm barrier filter with a pump wavelength of 880 nm at 80 femtosecond pulse width. A constant step size Z-section interval of 1.5  $\mu\text{m}$  was used across all Z-stack images collected. All parameters including detector gain, offset and laser power were kept constant to enable quantification. Images were processed using ImageJ software (version windows 64 bit, Fiji) and Imaris 9.5.0. High resolution images were taken on the Zeiss LSM 980 with an Airyscan 2 microscope (Zeiss) with x42 magnification and identical excitation/emission wavelengths for DAPI and  $\alpha\text{SMA}$ .

## 2.7 | Confocal image quantification

The immunostaining confocal imaging technique was used to detect  $\alpha\text{SMA}$  expressing myofibroblasts with an antibody that recognised the Cx43 molecule. Cx43 levels were quantitatively evaluated per tissue area and per cell nuclei in preterm AM specimens, using a well-established pixel-counting method, as previously described.<sup>35,36</sup> Maximum projections were performed in the AM to detect Cx43 levels expressed by cells present in the epithelial and fibroblast layers. The images were converted to binary using identical threshold values and objects exceeding 2 pixels were counted to identify Cx43-positive pixels per tissue area (500  $\mu\text{m}^2$ ) or per cell type. To quantify nuclei roundness, maximum RGB projections of the DAPI signal were converted to binary and using the particle measurement feature in ImageJ (Fiji) software, circularity values of nuclei defined by  $4\pi^*\text{area}/\text{perimeter}^2$  were calculated. Nuclear circularity analysis shows that a value of 1 indicates a perfect circle and reduces when the nucleus becomes increasingly elongated. To determine the direction of collagen alignment, SHG images were converted to binary and the 2D orientation analysis was performed using the local gradient orientation method and Directionality ImageJ plug-in (v2). This software calculates the number of objects that are distributed between either 0° and 180° or -90° and 90°, depending on the image direction of collagen fibres with a bin size of 1°.

## 2.8 | Biochemical analysis

The biochemical assays have described previously.<sup>21,35</sup> Briefly, DNA, GAG and collagen concentrations were measured by Hoechst 33,258, 1,9-dimethylmethylene blue and hydroxyproline assays (all reagents from Sigma-Aldrich Chemical Company). Elastin concentration was determined by the fastin elastin dye-binding method (Biocolor Life Science Assays).  $\text{PGE}_2$  release was determined by immunoassay (R&D Systems, Europe Ltd).

## 2.9 | Quantitative PCR

The methods for RNA extraction, cDNA synthesis and RT-qPCR have been described previously.<sup>35,36</sup> Primer pair sequences for Cx43 sense: 5'-CTGCCTATGTCTCCTCTG-3', antisense: 5'-TTGCTCA

CTTGCTTGCTTGT-3',  $\text{TGF}\beta_1$  sense: 5'-CCCAGCATCTGCAAAG CTC-3' and antisense: 5'-GTCAATGTACAGCTGCCGCA-3' and GAPDH sense: 5'-TCTCTGCTCCTCCTGTTC-3', GAPDH antisense: 5'-CGCCCAATACGACCAAAT-3'. PCR products were detected on the StepOnePlus Real-Time PCR System (ThermoFisher Scientific), as described<sup>21,35,36</sup> Relative gene quantification of Cx43 or  $\text{TGF}\beta_1$  was calculated by normalising the target to the reference gene, GAPDH and to the calibrator sample by a comparative Ct approach and ratio values expressed on a logarithmic scale.

## 2.10 | Statistical analysis

All values are expressed as the mean and  $\pm\text{SEM}$ . Statistical analysis was performed by a two-way analysis of variance (ANOVA) and the multiple post hoc Bonferroni corrected t-tests to compare differences between controls (no defect) and traumatised groups in CAM and PAM specimens. In all cases, values of  $p < 0.05$  were considered statistically significant. The number of replicates for each test condition from separate donors are indicated in the figure legend.

## 3 | RESULTS

### 3.1 | Cellular and collagen changes in preterm AM defects

Figure 1 shows a layer of  $\alpha\text{SMA}$  expressing myofibroblasts in the epithelial layer of preterm AM defects (green, Figure 1A). In the fibroblast layer, we observed a dense region of collagen and the presence of fibres across the defect site (red, Figure 1B). We observed the presence of myofibroblasts (blue) on either side of the wound (Figure 1B,C) and expressed Cx43 (Figure 1C, pink). In preterm AM defects subjected to mechanical stimulation, the direction of applied strain is shown with an arrow (Figure 1D–F). In the epithelial layer of preterm defects, mechanical stimulation increased cellularity of  $\alpha\text{SMA}$  expressing myofibroblasts (Figure 1D,F). In the fibroblast layer, the collagen fibres were dense (Figure 1E) and myofibroblasts expressed Cx43 (Figure 1F).

### 3.2 | Collagen organisation in preterm AM defects

Figure 2 examined the effects of mechanical stimulation on collagen directionality in preterm AM defects by SHG imaging. In control CAM and PAM specimens, collagen fibres appeared interwoven in a random fashion and had shorter basket-shaped fibres without polarity (Figure 2A,E). After mechanical stimulation, collagen fibres appeared dense and had high alignment, as shown by the dominant peak at 100° angle (Figure 2B,F). In preterm AM defects, the direction of collagen fibres was anisotropic with the angle of polarisation clearly distributed at 100° (Figure 2C,G). After mechanical stimulation, the fibres appeared denser and aligned tangentially to

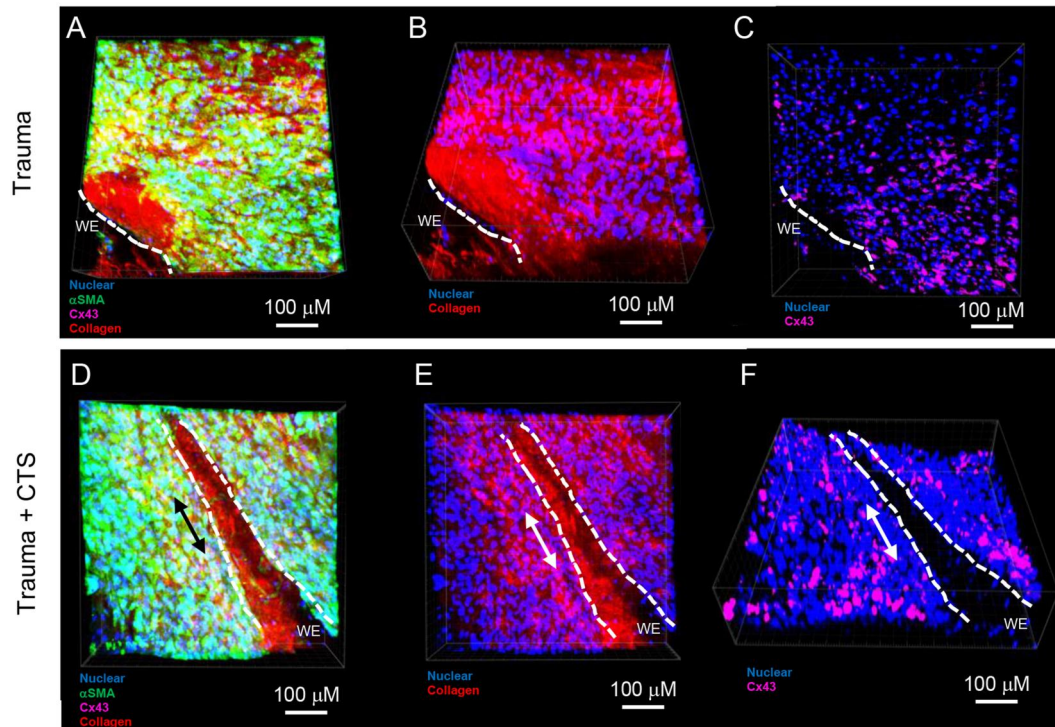


**FIGURE 1** Effects of mechanical stimulation in human preterm amniotic membrane (AM) defects. Preterm AM explants were traumatised with a needle to create a 0.8 mm defect and subjected to cyclic tensile strain (Trauma + CTS). Mechanical stimulation was applied intermittently at 2% strain and 1 Hz frequency for 24 h. At the end of the experiment, specimens were immunostained to detect Cx43 and  $\alpha$ SMA in myofibroblasts. Signals for blue (DAPI), green ( $\alpha$ SMA), pink (Cx43) and red (collagen) were detected by immunofluorescence confocal microscopy and second harmonic generation (SHG) imaging. The dotted white lines show the wound edge (WE) in the preterm AM specimen (scale bar = 100  $\mu$ m, left panel). Representative confocal and SHG images are shown from one late third trimester fetal growth restricted (FGR) donor (35 + 5 weeks). [Colour figure can be viewed at [wileyonlinelibrary.com](http://wileyonlinelibrary.com)]

the wound edge (Figure 2D,H). The level of polarity was similar for the experimental test conditions but different from control specimens (Figure 2A,E), demonstrating that mechanical stimulation influences the spatial orientation of collagen fibres in preterm AM defects.

### 3.3 | Nuclei deformation in preterm AM defects

The effects of mechanical stimulation on nuclei morphology are shown in Figure 3. In preterm AM subjected to mechanical stimulation, the majority of cells in the epithelial and fibroblast layers had elongated morphologies (white arrow, Figure 3A) and at high magnification appeared to be aligned in the direction of applied strain (Figure 3B,C). Cells were observed to form clusters around the wound edge (Figure 3D) and the nuclei appeared deformed (Figure 3E,F) in preterm AM defects. We next quantified the roundness of the nuclear shape (inset, Figure 2). In preterm AM, mechanical stimulation significantly reduced values for nuclei circularity in AECs from  $0.75 \pm 0.016$  to  $0.38 \pm 0.013$  and in AMCs/myofibroblasts from  $0.87 \pm 0.002$  to  $0.54 \pm 0.012$  ( $p < 0.001$ , inset Figure 3). Both trauma and mechanical stimulation reduced nuclei circularity values further ranging from  $0.44 (\pm 0.02)$  and  $0.47 (\pm 0.01)$  in AECs and AMCs/myofibroblasts, respectively, when compared to

controls ( $0.76 \pm 0.015$  and  $0.88 \pm 0.002$ ). Quantification by nuclei circularity analysis demonstrated that mechanical stimulation in preterm AM defects reduced nuclear roundness, indicating an increasingly elongated nuclei shape.

### 3.4 | Cx43 protein expression in preterm AM defects

In the absence and presence of trauma, mechanical stimulation significantly increased Cx43 protein expression in the epithelial and fibroblast layer of CAM specimens (all  $p < 0.001$ ; Figure 4A). Co-stimulation with CTS and Cx43 antisense abolished this response (all  $p < 0.001$ ; Figure 4A). A similar trend was found in the epithelial layer of PAM specimens, where mechanical stimulation increased Cx43 values from 130 to 1542 pixels/500  $\text{cm}^2$  after trauma ( $p < 0.001$ , Figure 4A). However, in the fibroblast layer of PAM specimens, mechanical stimulation significantly reduced Cx43, but in PAM defects, values increased from 391 to 871 pixels/500  $\text{cm}^2$  (all  $p < 0.001$ , Figure 4A). In all test conditions, co-treatment with Cx43 antisense abolished the response with values ranging from 0.8 to 10 pixels/500  $\text{cm}^2$  (all  $p < 0.001$ , Figure 4A). In CAM specimens, AECs and myofibroblasts expressed broadly similar values of Cx43 than PAM, but levels were higher in myofibroblasts than AECs (both



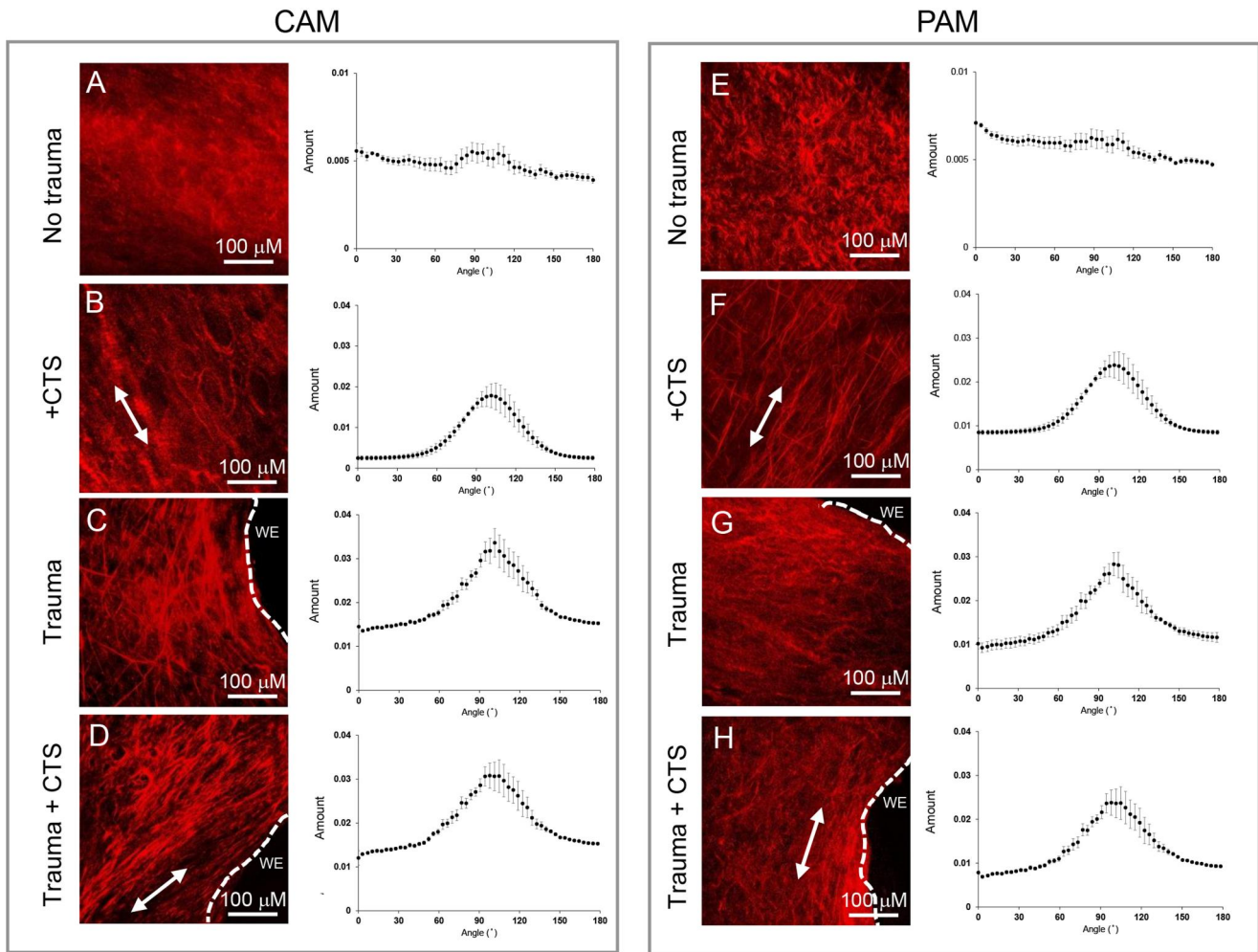


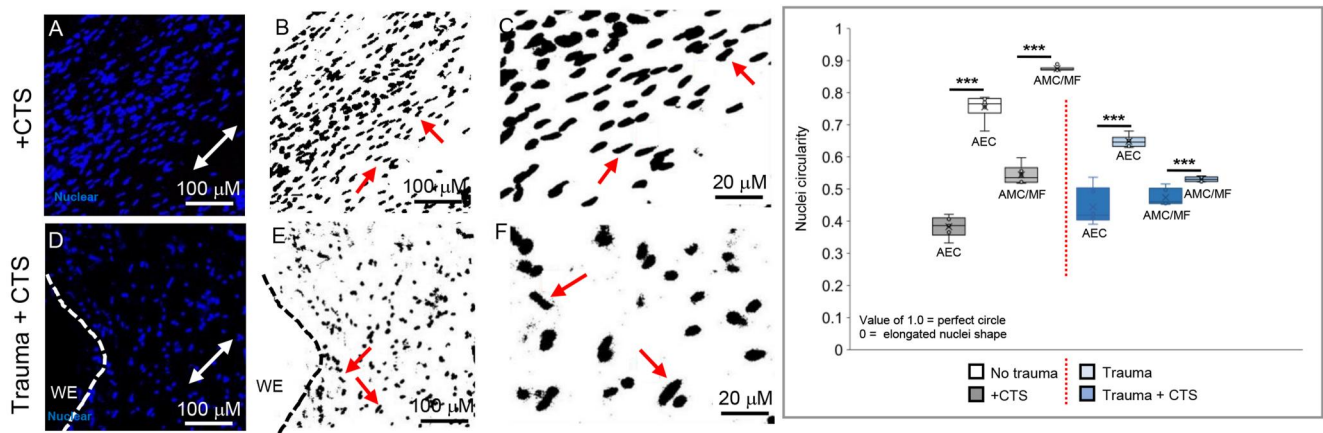
**FIGURE 2** Effects of mechanical stimulation on collagen organisation in preterm amniotic membrane (AM) defects. The organisation of the collagen fibres in AM specimens close to the cervix (CAM) or placenta (PAM) was detected by second harmonic generation (SHG) microscopy. Specimens were traumatised with a needed to create a 0.8 mm defect and subjected to 2% cyclic tensile strain (CTS) for 24 h. SHG imaging of the collagen fibres appeared as red signals. The dotted white lines show the length of the wound edge (WE) and white arrows the direction of applied strain. Representative SHG images are shown for one field of view, where scale bar = 100  $\mu\text{m}$ . Analysis of the direction of collagen fibres at a specific polarisation angle is shown in the alignment graphs. Error bars represent the analysis of collagen fibre alignment in three regions and analysis repeated with six replicates taken from three late third trimester fetal growth restricted (FGR) donors (33 + 0 weeks to 35 + 6 weeks). [Colour figure can be viewed at [wileyonlinelibrary.com](https://onlinelibrary.wiley.com/doi/10.1002/pd.6429)]

$p < 0.001$ , Figure 4B). In PAM defects, AECs but not myofibroblasts increased Cx43 expression and the response was enhanced by mechanical stimulation but abolished with the antisense (all  $p < 0.001$ , Figure 4B).

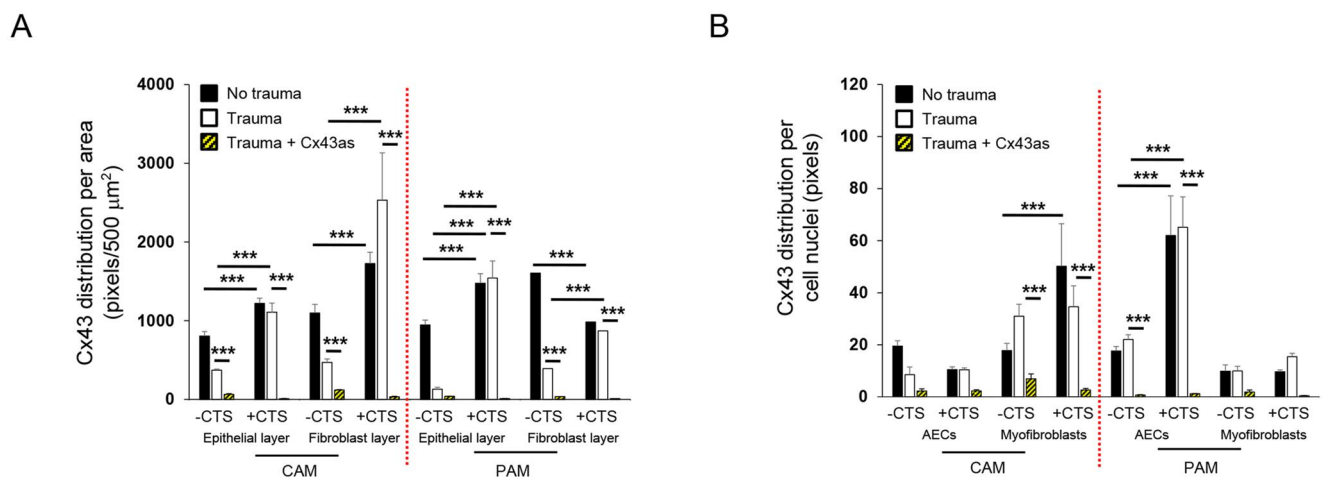
### 3.5 | Effects of mechanical stimulation in singleton and twin preterm AM defects

Figure 5 examined the effects of mechanical stimulation in preterm CAM and PAM specimens from singleton and twin pregnancies on the levels of GAG (A), collagen (B), elastin (C) and PGE<sub>2</sub> (D). In control singleton specimens (no trauma), CTS increased GAG content (both  $p < 0.001$ , Figure 5A) with a greater magnitude of stimulation in CAM (114.1%) than PAM (44.9%). After trauma, GAG content reduced in

CAM but not in PAM and co-treatment with CTS and the Cx43 antisense reduced GAG content. In control twin specimens, the magnitude of stimulation by CTS was greater in PAM (225.7%) than in CAM (43.8%). Trauma increased GAG content in PAM ( $p < 0.01$ ) but not in CAM and the response was abolished with the antisense ( $p < 0.01$ ). In control specimens, absolute values for collagen content were broadly similar and ranged from 6.76 to 9.36  $\mu\text{g}/\text{mg}$  (Figure 5B). After trauma, CTS significantly reduced collagen in singleton (both  $p < 0.001$ ) but not twin specimens and the response was reversed after co-stimulation with CTS and Cx43 antisense ( $p < 0.001$ ). In controls, CTS significantly increased elastin content in singleton (both  $p < 0.001$ , Figure 5C) but not twin specimens. After trauma, CTS reduced elastin content and the effects were reversed with the antisense (Figure 5C). Values for PGE<sub>2</sub> release were broadly similar, ranging from 4.92 to 9.48 ng/mL in singleton and twin specimens.



**FIGURE 3** Effects of mechanical stimulation on nuclei morphology. Nuclei shape were quantified in preterm amniotic membrane (AM) defects subjected to cyclic tensile strain (CTS) for 24 h. Specimens were imaged in the epithelial and fibroblast layers to detect cell types by immunofluorescence confocal microscopy. Maximum RGB projections of the DAPI signal (blue nuclei) were converted to binary images and nuclei circularity values calculated using the particle measurement feature in the ImageJ software, where scale bar = 20 and 100  $\mu\text{m}$ . Box and whisker plots represent values for ~200–250 cells measured in AM ( $n = 6$  specimens) from three late third trimester fetal growth restricted (FGR) donors (33 + 0 weeks to 35 + 6 weeks). [Colour figure can be viewed at [wileyonlinelibrary.com](http://wileyonlinelibrary.com)]



**FIGURE 4** Effects of mechanical stimulation on Cx43 protein expression in preterm amniotic membrane (AM) defects. Explants isolated from the cervix (CAM) or placenta (PAM) regions were traumatised with a needle to create a 0.8 mm defect and subjected to cyclic tensile strain (+CTS) for 24 h, in the presence and absence of Cx43 antisense (Cx43as). The distribution of Cx43 was analysed per tissue area for comparisons between the epithelial and fibroblast layers (A) and AECs or myofibroblast cell nuclei (B). Error bars represent the mean and SEM values of 6 replicates from three late trimester fetal growth restricted (FGR) donors (33 + 0 weeks to 35 + 6 weeks), where \*\*\* $p < 0.001$  indicates significant comparisons for no cyclic tensile strain (–CTS) or + CTS conditions. All other comparisons (not indicated) were not significantly different. AECs, Amniotic Epithelial Cells. [Colour figure can be viewed at [wileyonlinelibrary.com](http://wileyonlinelibrary.com)]

### 3.6 | Effects of mechanical stimulation in early and late sPPROM

Figure 6 examined absolute values for GAG, collagen, elastin and  $\text{PGE}_2$  release from sPPROM donors who delivered early preterm ( $\leq 32$  weeks gestation) or late preterm ( $\geq 32$  weeks gestation). In early but not late sPPROM, CTS increased GAG content in PAM ( $p < 0.001$ ) but not in CAM specimens and this response was reduced by the Cx43 antisense ( $p < 0.001$ ; Figure 6A). In CAM but not PAM

specimens, CTS reduced collagen content from early and late sPPROM and reversed with Cx43 antisense in CAM and PAM defects (all  $p < 0.001$ ; Figure 6B). In early sPPROM specimens, absolute values for elastin content were broadly similar but in late sPPROM, CTS and Cx43 antisense increased values in CAM but not PAM ( $p < 0.001$ , Figure 6C). Additionally, values for  $\text{PGE}_2$  release ranged from 9.7 to 11.1 ng/mL in early and late sPPROM specimens (Figure 6D) and was reduced by Cx43 antisense to  $< 2.5$  ng/mL in late sPPROM specimens only.

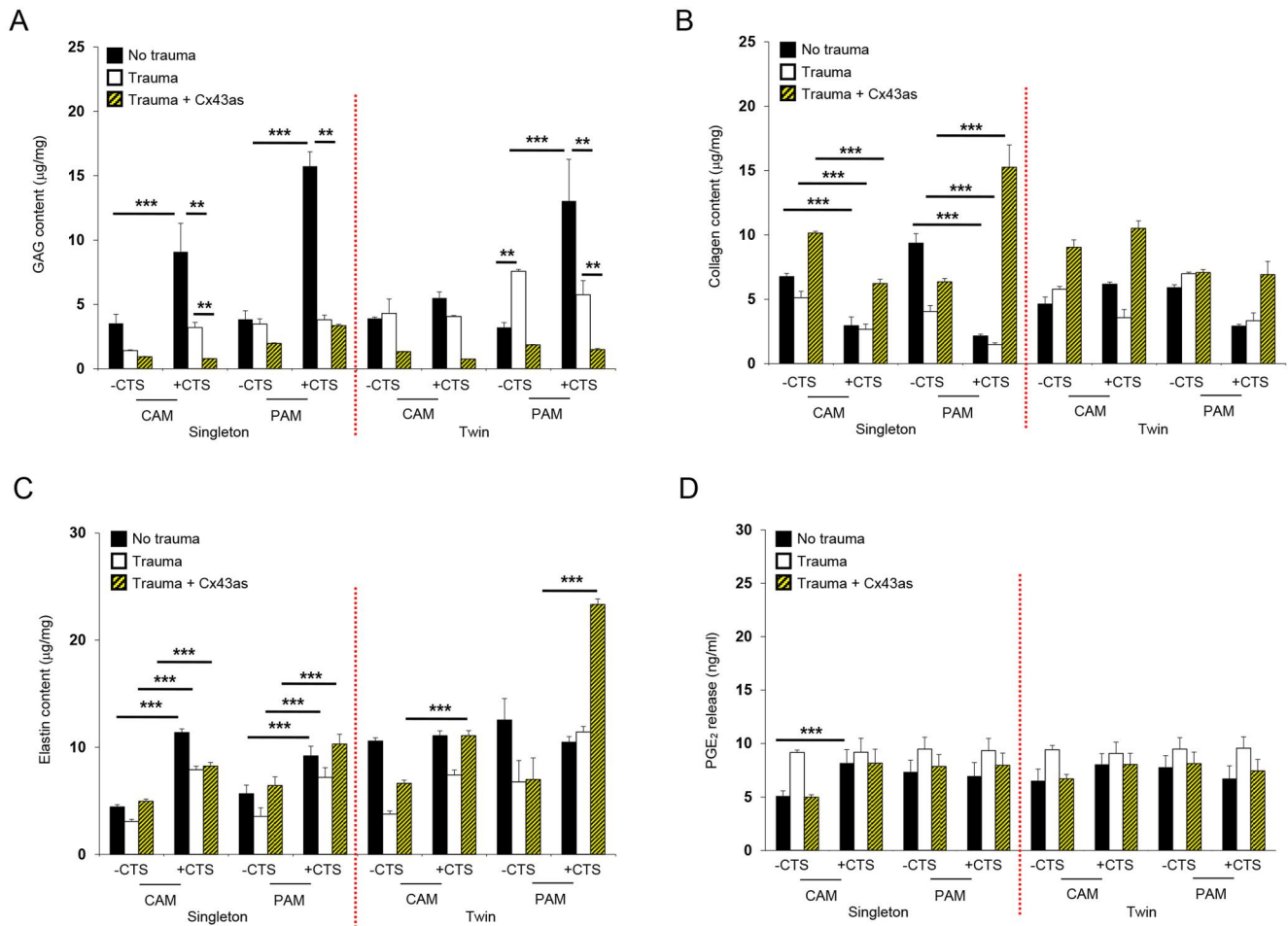


**FIGURE 5** Effects of mechanical stimulation in singleton and twin preterm amniotic membrane (AM) defects. Explants isolated from the cervix (CAM) or placenta (PAM) regions were traumatised with a needed to create a 0.8 mm defect and subjected to cyclic tensile strain (+CTS) for 24 h. Mechanical stimulation was applied intermittently at 2% strain and 1 Hz frequency in the presence and absence of 50 µM Cx43 antisense (Cx43as). Absolute values for GAG (A), collagen (B) and elastin content were normalised to dry tissue weight (C). PGE<sub>2</sub> release was quantified in media samples (D). Explants cultured without cyclic tensile strain (–CTS) were compared to +CTS specimens. Error bars represent the mean and SEM values of 9–12 replicates from four early or three late trimester fetal growth restricted (FGR) donors, where \*\* $p < 0.01$  or \*\*\* $p < 0.001$  indicates significant comparisons for –CTS and +CTS conditions. All other comparisons (not indicated) were not significantly different. [Colour figure can be viewed at [wileyonlinelibrary.com](https://onlinelibrary.wiley.com/terms-and-conditions)]

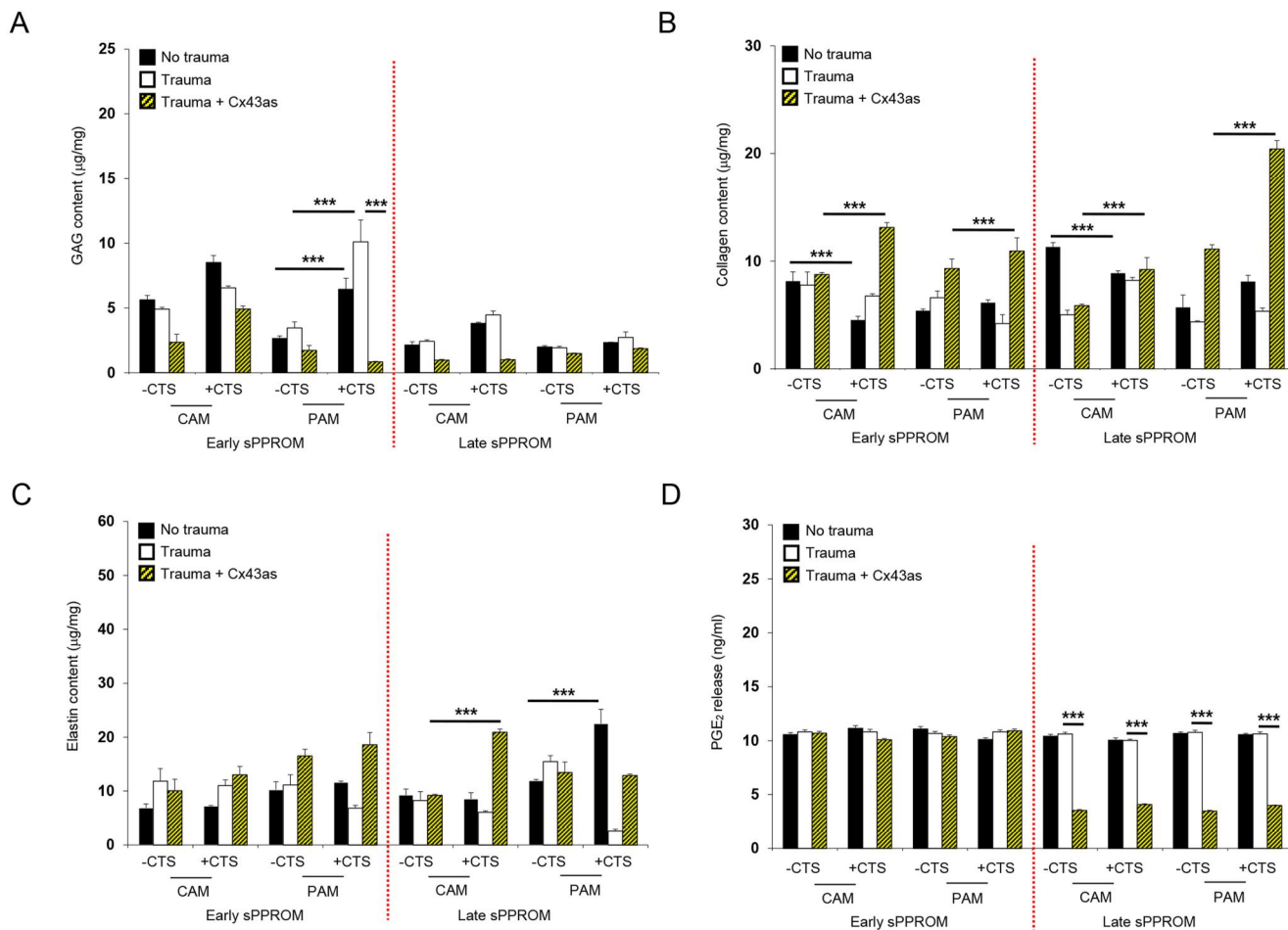
### 3.7 | Effects of mechanical stimulation on gene expression

Figure 7 examined the effects of mechanical stimulation on Cx43 and TGFβ gene expression in preterm AM defects. In CAM but not PAM specimens from early sPPROM donors, CTS increased Cx43 gene expression and this response was abolished with antisense ( $p < 0.001$ , Figure 7A). In late sPPROM specimens, trauma and mechanical stimulation increased Cx43 gene expression in CAM and PAM specimens and was reduced by the antisense. In early sPPROM, mechanical stimulation increased TGFβ<sub>1</sub> gene expression in CAM and PAM defects and was further enhanced with Cx43 antisense. In late sPPROM, mechanical stimulation significantly increased TGFβ<sub>1</sub> gene expression in CAM defects ( $p < 0.001$ , Figure 6B) but not in PAM defects and was reduced by co-treatment with Cx43 antisense.

## 4 | DISCUSSION

It is well established that mechanical stimulation regulates the structure and function of fetal membranes by regulating signals to maintain tissue homeostasis during preterm gestation. As the tissue approach term, the onset and progression of collagen remodelling is required to break down the extracellular matrix, facilitate cross-talk with inflammatory cascades and weaken the fetal membranes. We previously showed that during wound healing in term AM, Cx43 upregulates AMCs to form plaques between cells and is a mechanism which prevents migration and healing of the wound. This process is synchronous to AMC differentiation also induced by Cx43, where myofibroblasts migrate to the defect site, synthesise collagen and contract the edges of the wound via a purse-string mechanism. Both TGFβ and Cx43 facilitate wound healing mechanisms and form functional gap junctions and hemichannels which are critical for mechanotransduction,





**FIGURE 6** Effects of mechanical stimulation on early and late preterm AM defects. Preterm AM explants isolated from the cervix (CAM) or placenta (PAM) regions were traumatised with a needle to create a 0.8 mm defect and subjected to cyclic tensile strain (+CTS) for 24 h. Mechanical stimulation was applied intermittently at 2% strain and 1 Hz frequency in the presence and absence of 50 µM Cx43 antisense (Cx43as). Absolute values for GAG (A), collagen (B) and elastin content were normalised to dry tissue weight (C). PGE<sub>2</sub> release was quantified in media samples (D). Explants cultured without cyclic tensile strain (-CTS) were compared to +CTS specimens. Error bars represent the mean and SEM values of 8–12 replicates from early trimester sPPROM donors ( $n = 2$ , 27–31 weeks gestation) or late trimester sPPROM donors ( $n = 3$ ,  $\geq 32$  weeks gestation). Significant comparisons are indicated for -CTS and +CTS conditions where  $**p < 0.01$  or  $***p < 0.001$ . All other comparisons (not indicated) were not significantly different. AM, amniotic membrane. [Colour figure can be viewed at [wileyonlinelibrary.com](https://onlinelibrary.wiley.com/terms-and-conditions)]

differentiation, inflammation and repair.<sup>37–39</sup> However, the imbalance of matrix synthesis is coordinated by catabolic activities resulting in increased cytokines, prostaglandins and MMPs which can hinder repair mechanisms in human fetal membranes.<sup>1–3,7,9</sup> The present study enables the investigation of mechanical stimulation on cell behaviour, collagen organisation and protein expression in preterm AM defects. We explored the effects of iatrogenic preterm birth, sPPROM and multiple pregnancies in groups of donors to better understand the different mechanisms underlying PPROM and the apparent failure of the AM to heal. Importantly, we examined the combined effects of mechanical stimulation and Cx43 antisense in AM defects on markers for inflammation, matrix and repair.

In preterm AM defects, mechanical stimulation showed a dense, thicker region of fibres aligned tangentially to the wound edge and could be early signs of wound contraction similar to a healing response that we previously quantified in term AM.<sup>35,36,40</sup> The direction of collagen fibres was identical with a polarisation angle at

100°C in preterm AM defects from FGR donors and showed a similar response in term AM defects, demonstrating the spatial organisation and movement of collagen fibres between cell and matrix layers.<sup>35</sup> Additionally, nuclei roundness is influenced by the viscoelastic nature of collagen where hydration and tissue volume increase the tension and creep response with mechanical strain enabling tissue recovery without permanent deformation.<sup>34,41–43</sup> Whilst the biomechanical behaviour of term human AM is well documented, the deformation response of collagen fibres in preterm AM with tissue region is less clear.<sup>30,41,44</sup> We did not quantify the diameter of collagen fibres with axial order, which could be a reason for structural changes at the molecular scale, particularly with inhomogeneous orientations with gestational age or disease. Further investigations involving small-angle X-ray scattering, which explores fibre thickness, length and directionality to assess differences in spatial and temporal organisation could be explored. Additionally, multiple cell types in AM defects were deformed after mechanical stimulation. It is not clear if

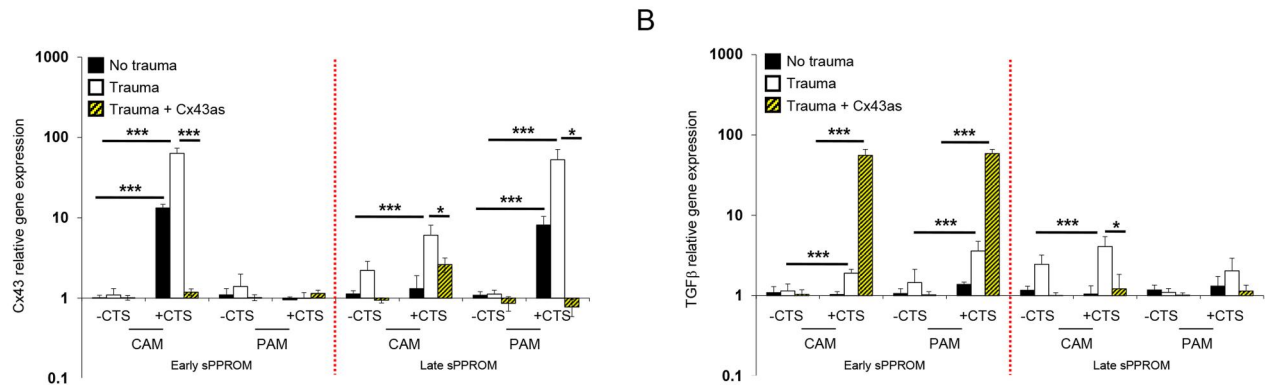


**FIGURE 7** Effects of mechanical stimulation on gene expression in preterm amniotic membrane (AM) defects. Explants isolated from the cervix (CAM) or placenta (PAM) regions were traumatised with a needed to create a 0.8 mm defect and subjected to cyclic tensile strain (+CTS) for 24 h. Mechanical stimulation was applied intermittently at 2% strain and 1 Hz frequency in the presence and absence of 50  $\mu$ M Cx43 antisense (Cx43as). Gene expression of Cx43 (A) and Transforming Growth Factor  $\beta$  (TGF $\beta$ ) (B) in CAM and PAM specimens are presented as ratio values and normalised to control values. In all cases, error bars represent the mean and SEM values of 12–18 replicates, where (\*, \*\* or \*\*\*) indicates significant comparisons for –CTS and +CTS CAM or PAM conditions. All other comparisons (not indicated) were not significantly different. [Colour figure can be viewed at [wileyonlinelibrary.com](https://onlinelibrary.wiley.com/doi/10.1002/pd.6429)]

there is a difference in reversible transition rates between AEC and AMC to myofibroblast morphology in preterm AM defects contributing to differences in Cx43 concentration in the epithelial and fibroblast layer, as found previously.<sup>32,40,45</sup> In small mouse defects, AECs undergo EMT, enabling a migratory cell population that can heal defects.<sup>28,29</sup> The role of EMT transition and the purse-string contraction hypothesis after mechanical stimulation in preterm AM defects should be explored further.

In term AM, cells respond to stretch by activating inflammatory cytokines, PGE<sub>2</sub> production and MMPs that degrade collagen and weaken the membrane prior to rupture.<sup>12–19</sup> In the present study, we explored the effects of mechanical stimulation on protein synthesis in preterm AM. Whilst it is difficult to interpret the biochemical data and compare the effects with specimens analysed from a small number of donors, absolute values in the same donor were consistent, demonstrating the strength of the biomechanical model system, which is well known to be dependent on the magnitude, duration and nature of the mechanical stimulus. The donor to donor variability for each group demonstrates variations in patient data sets due to the effects of disease or maternal and gestational age. In a comparison of how the mechanical environment affects membrane integrity with other studies, uterine overdistention in twin pregnancies demonstrates greater tissue weakening mechanisms and higher levels of oxytocin and markers for inflammation.<sup>8,46–49</sup> In AM specimens, tensile stretching increased Cx43, COX-2 and the oxytocin receptor leading to enhanced cytokine production, resulting in reduced tensile strength and greater susceptibility to rupture, whilst in rat myometrium, Cx43 was reported to increase after stretch.<sup>12,18,20</sup> In the FGR group where we compared singleton and twin deliveries, PGE<sub>2</sub> concentrations were high (>10 ng/mL) compared to values we found previously (<1 ng/mL) in term AM, leading to inflammatory mechanisms, apoptosis and possible uterine contractions.<sup>49–52</sup> Whilst there are limitations with the current study, apoptosis triggered by PGE<sub>2</sub> and repetitive stretch could enhance oxidative and mechanical stress mechanisms, softening and early rupture.<sup>11</sup> In contrast, the

implications of Cx43 and TGF $\beta$ <sub>1</sub> signalling to heal preterm AM defects could be a protective mechanism to enhance differentiation, migration and repair, but the pathways need to be investigated further with appropriate 3D models.<sup>4,9,12,53–57</sup>

## 5 | CONCLUSION

In summary, mechanical stimulation increased nuclei deformation and collagen polarity in preterm AM defects. Whilst mechanical stimulation increased Cx43 in AECs and myofibroblasts, this response was dependent on tissue type, with differences in protein expression between CAM and PAM specimens. In preterm AM defects, mechanical stimulation promotes structural changes in collagen that increase polarity and potentially could promote wound contraction via a purse string mechanism as identified previously.<sup>35,36,40</sup> Whilst the present study did not quantify closure at the defect site, we observed the presence of myofibroblasts in and around the defect site which activate TGF $\beta$ <sub>1</sub> and healing, as described by others.<sup>55,56</sup> A combination of inflammatory and mechanical factors may perturb typical mechanotransduction processes mediated by Cx43 and was rescued after Cx43 knockdown. Whilst matrix molecules were influenced by mechanical stimulation, it was difficult to interpret the biochemical data and compare the effects with specimens analysed from a small number of donors from three classification groups. In the future, it will be necessary to consider how gestational age, the number of pregnancies and disease affect the design of experiments. Our understanding of how inflammation affects the microstructure and mechanical strength of fetal membranes is limited due to the lack of pre-clinical models that replicate the 3D microenvironment. Whilst there has been progress in microfluidic models of placenta using organ-on-a-chip technology, fetal membrane models that replicate the mechanical environment have been neglected. This multi-layered tissue is bathed in amniotic fluid and subjected to unique mechanical forces during pregnancy. In

vitro models must combine biological and engineering approaches, enabling researchers to provide meaningful information on membrane physiology and wound healing mechanisms in human preterm and term tissues for PPROM prevention.

## ACKNOWLEDGEMENTS

The authors thank the National Institute for Health Research at the University College London Hospitals Biomedical Research Centre. ALD is supported by the NIHR UCLH Biomedical Research Centre. This work was supported by GOSH Medical Charity (17QMU01, TTC), Rosetrees Trust (M808, TTC), KU Leuven University Fund (JD) and the Prenatal Therapy Fund, University College London Hospital Charity (ALD).

## CONFLICT OF INTEREST STATEMENT

The authors report no conflicts of interest and no financial interest.

## DATA AVAILABILITY STATEMENT

The data that support the findings of this study are available from the corresponding author upon request.

## ORCID

Jan A. Deprest  <https://orcid.org/0000-0002-4920-945X>

Anna L. David  <https://orcid.org/0000-0002-0199-6140>

Tina T. Chowdhury  <https://orcid.org/0000-0003-4167-7782>

## REFERENCES

- Kumar D, Moore R, Mercer B, Mansour JM, Redline RW, Moore JJ. The physiology of fetal membrane weakening and rupture: insights gained from the determination of physical properties revisited. *Placenta*. 2016;42:59-73. <https://doi.org/10.1016/j.placenta.2016.03.015>
- Menon R, Behnia F, Poletini J, Richardson L. Novel pathways of inflammation in human fetal membranes associated with preterm birth and preterm pre-labor rupture of the membranes. *Seminars Immunopathol*. 2020;42(4):431-450. <https://doi.org/10.1007/s00281-020-00808-x>
- Pressman E, Cavanaugh J, Woods J. Physical properties of the chorioamnion throughout gestation. *Am J Obstet Gynecol*. 2002;187(3):672-675. <https://doi.org/10.1067/mob.2002.125742>
- Gratacós E, Sanin-Blair J, Lewi L, et al. A histological study of fetoscopic membrane defects to document membrane healing. *Placenta*. 2006;27(4-5):452-466. <https://doi.org/10.1016/j.placenta.2005.03.008>
- Oyen M, Calvin S, Landers D. Premature rupture of the fetal membranes: is the amnion the major determinant? *Am J Obstet Gynecol*. 2006;195(2):510-515. <https://doi.org/10.1016/j.ajog.2006.02.010>
- Oyen M, Cook R, Calvin S. Mechanical failure of human fetal membrane tissues. *J Mater Sci Mater Med*. 2004;15(6):651-658. <https://doi.org/10.1023/b:jmsm.0000030205.62668.90>
- McLaren J, Taylor D, Bell S. Increased concentration of pro-matrix metalloproteinase 9 in term fetal membranes overlying the cervix before labor: implications for membrane remodeling and rupture. *Am J Obstet Gynecol*. 2000;182(2):409-416. [https://doi.org/10.1016/s0002-9378\(00\)70232-8](https://doi.org/10.1016/s0002-9378(00)70232-8)
- Adams WK, Singh N, Mohan A, et al. Uterine overdistention induces preterm labor mediated by inflammation: observations in pregnant women and nonhuman primates. *Am J Obstet Gynecol*. 2015;213(6):830.e1-830.e19. <https://doi.org/10.1016/j.ajog.2015.08.028>
- Mogami H, Kishore HA, Akgul Y, Word R. Healing of preterm ruptured fetal membranes. *Sci Rep*. 2017;7(1):13139. <https://doi.org/10.1038/s41598-017-13296-1>
- Borazjani A, Weed B, Patnaik S, et al. A comparative biomechanical analysis of term fetal membranes in human and domestic species. *Am J Obstet Gynecol*. 2011;204(4):365.e25-365.e36. <https://doi.org/10.1016/j.ajog.2010.12.003>
- Amberg B, Hodges R, Rodgers K, Crossley KJ, Hooper SB, DeKoninck PL. Why do the fetal membranes rupture early after fetoscopy? ZA review. *Fetal Diagn Ther*. 2021;48(7):493-503. <https://doi.org/10.1159/000517151>
- Kumar D, Moore RM, Mercer BM, Mansour JM, Moore JJ. Mechanism of human fetal membrane biomechanical weakening, rupture and potential targets for therapeutic intervention. *Obstet Gynecol Clin N Am*. 2020;47(4):523-544. <https://doi.org/10.1016/j.jogc.2020.08.010>
- Richardson L, Vargas G, Brown T, et al. Discovery and characterization of human amniochorionic membrane microfractures. *Am J Pathol*. 2017;187(12):2821-2830. <https://doi.org/10.1016/j.ajpath.2017.08.019>
- Richardson L, Radnaa E, Urrabaz-Garza R, Lavu N, Menon R. Stretch, scratch, and stress: suppressors and supporters of senescence in human fetal membranes. *Placenta*. 2020;99:27-34. <https://doi.org/10.1016/j.placenta.2020.07.013>
- Mohan AR, Soorranna SR, Lindstrom TM, Johnson MR, Bennett PR. The effect of mechanical stretch on cyclooxygenase type 2 expression and AP-1 and NF-κB activity in human amnion cells. *Endocrinology*. 2007;148(4):1850-1857. <https://doi.org/10.1210/en.2006-1289>
- Kanayama N, Fukamizu H. Mechanical stretching increases PGE<sub>2</sub> in cultured human amnion cells. *Gynecol Obstet Invest*. 1989;28(3):123-126. <https://doi.org/10.1159/000293546>
- Maehara K, Kanayama N, Maradny EE, Uezato T, Fujita M, Terao T. Mechanical stretching induces IL-8 gene expression in fetal membranes: a possible role for the initiation of human parturition. *Eur J Obstet Gynecol Reprod Biol*. 1996;27(2):191-196. [https://doi.org/10.1016/s0301-2115\(95\)02602-9](https://doi.org/10.1016/s0301-2115(95)02602-9)
- Ou CW, Orsino A, Lye SJ. Expression of Cx43 and Cx26 in the rat myometrium during pregnancy and labor is differentially regulated by mechanical and hormonal signals. *Endocrinology*. 1997;138(12):5398-5407. <https://doi.org/10.1210/endo.138.12.5624>
- Mohan AR, Sooranna SR, Lindstrom TM, Johnson MR, Bennett PR. The effect of mechanical stretch on COX2 expression and AP-1 and NFκB activity in human amnion cells. *Endocrinology*. 2007;148(4):1850-1857. <https://doi.org/10.1210/en.2006-1289>
- Kendal-Wright CE. Stretching, mechanotransduction, and proinflammatory cytokines in the fetal membranes. *Reprod Sci*. 2007;14(S8):35-41. <https://doi.org/10.1177/1933719107310763>
- Chowdhury B, David A, Thrasivoulou C, Becker D, Bader D, Chowdhury T. Tensile strain increased COX-2 expression and PGE<sub>2</sub> release leading to weakening of the human amniotic membrane. *Placenta*. 2014;35(12):1057-1064. <https://doi.org/10.1016/j.placenta.2014.09.006>
- Richardson L, Jeong S, Kim S, Hart A, Menon R. Amnion membrane organ-on-chip: an innovative approach to study cellular interactions. *FASEB J*. 2019;33(8):8693-9695. <https://doi.org/10.1096/fj.201900020rr>
- Richardson L, Kim S, Menon R, Han A. Organ-On-Chip Technology: the future of feto-maternal interface research? *Front Physiol*. 2020;11:715. <https://doi.org/10.3389/fphys.2020.00715>
- El Maradny E, Kanayama N, Halim A, Maehara K, Terao T. Stretching of fetal membranes increases the concentration of interleukin-8 and collagenase activity. *Am J Obstet Gynecol*. 1996;174(3):843-849. [https://doi.org/10.1016/s0002-9378\(96\)70311-3](https://doi.org/10.1016/s0002-9378(96)70311-3)
- Sasamoto A, Nagino M, Kobayashi S, Naruse K, Nimura Y, Sokabe M. Mechanotransduction by integrin is essential for IL-6 secretion from

- endothelial cells in response to uniaxial continuous stretch. *Am J Physiol Cell Physiol*. 2004;288(5):1012-1022. <https://doi.org/10.1152/ajpcell.00314.2004>
26. Nemeth E, Millar LK, Bryant-Greenwood GD. Fetal membrane distension II. Differentially expressed genes regulated by acute distension in vitro. *Am J Obstet Gynecol*. 2000;182(1):60-67. [https://doi.org/10.1016/s0002-9378\(00\)70491-1](https://doi.org/10.1016/s0002-9378(00)70491-1)
  27. Jabareen M, Mallik A, Bilic G, Zisch AH, Mazza E. Relation between mechanical properties and microstructure of human fetal membranes: an attempt towards a quantitative analysis. *Eur J Obstet Gynecol Reprod Biol*. 2009;144:S134-S141. <https://doi.org/10.1016/j.ejogrb.2009.02.032>
  28. Janzen C, Sen S, Lei M, Gagliardi de Assumpcao M, Challis J, Chaudhuri G. The role of epithelial to mesenchymal transition in human amniotic membrane rupture. *J Clin Endocrinol Metabol*. 2016;jc.2016-3150. <https://doi.org/10.1210/jc.2016-3150>
  29. de Castro Silva M, Richardson L, Kechichian T, et al. Inflammation, but not infection, induces EMT in human amnion epithelial cells. *Reproduction*. 2020;160(4):627-638.
  30. Perrini M, Mauri A, Ehret AE, et al. Mechanical and microstructural investigation of the cyclic behavior of human amnion. *J Biomech Eng*. 2015;137(6):061010. <https://doi.org/10.1115/1.4030054>
  31. Richardson LS, Kim S, Han A, Menon R. Modeling ascending infection with a feto-maternal interface organ-on-chip. *Lab Chip*. 2020;20(23):4486-4501. <https://doi.org/10.1039/d0lc00875c>
  32. Richardson L, Taylor R, Menon R. Reversible EMT and MET mediate amnion remodelling during pregnancy and labor. *Sci Signal*. 2020;13(618):eaay1486. <https://doi.org/10.1126/scisignal.aay1486>
  33. Buerzle W, Mazza E. On the deformation behavior of human amnion. *J Biomech*. 2013;46(11):1777-1783. <https://doi.org/10.1016/j.jbiomech.2013.05.018>
  34. Mauri A, Perrini M, Mateos J, et al. Second harmonic generation microscopy of fetal membranes under deformation: normal and altered morphology. *Placenta*. 2013;34(11):1020-1026. <https://doi.org/10.1016/j.placenta.2013.09.002>
  35. Barrett DW, Kethees A, Thrasivoulou C, et al. Trauma induces overexpression of Cx43 in human fetal membrane defects. *Prenat Diagn*. 2017;37(9):899-906. <https://doi.org/10.1002/pd.5104>
  36. Costa E, Okesola BO, Thrasivoulou C, et al. Cx43 mediates changes in myofibroblast contraction and collagen release in human amniotic membrane defects after trauma. *Sci Rep*. 2021;11(1):16975. <https://doi.org/10.1038/s41598-021-94767-4>
  37. Mori R, Power K, Wang C, Martin P, Becker DL. Acute down-regulation of connexin 43 at wound sites leads to a reduced inflammatory response, enhanced keratinocyte proliferation and wound fibroblast migration. *J Cell Sci*. 2006;119(24):5193-5203. <https://doi.org/10.1242/jcs.03320>
  38. Montgomery J, Ghatnekar G, Grek C, Moyer K, Gourdie R. Connexin 43-based therapeutics for dermal wound healing. *Int J Mol Sci*. 2018;19(6):1778. <https://doi.org/10.3390/ijms19061778>
  39. Faniku C, O'Shaughnessy E, Lorraine C, et al. The connexin mimetic peptide Gap27 and Cx43-knockdown reveal differential roles for Connexin43 in wound closure events in skin model systems. *Int J Mol Sci*. 2018;19(2):604. <https://doi.org/10.3390/ijms19020604>
  40. Mogami H, Kishore A, Word R. Collagen type 1 accelerates healing of ruptured fetal membranes. *Sci Rep*. 2018;8(1):696. <https://doi.org/10.1038/s41598-017-18787-9>
  41. Mauri A, Perrini M, Ehret A, De Focatiis DS, Mazza E. Time-dependent mechanical behavior of human amnion: macroscopic and microscopic characterization. *Acta Biomater*. 2015;11:314-323. <https://doi.org/10.1016/j.actbio.2014.09.012>
  42. Buerzle W, Haller C, Jabareen M, et al. Multiaxial mechanical behaviour of human fetal membranes and its relationship to microstructure. *Biomech Model Mechanobiol*. 2012;12(4):747-762. <https://doi.org/10.1007/s10237-012-0438-z>
  43. Bircher K, Merluzzi R, Wahlsten A, et al. Influence of osmolarity and hydration on the tear resistance of the human amniotic membrane. *J Biomech*. 2020;98:109419. <https://doi.org/10.1016/j.jbiomech.2019.109419>
  44. Oyen M, Cook R, Stylianopoulos T, Barocas VH, Calvin SE, Landers DV. Uniaxial and biaxial mechanical behaviour of human amnion. *J Mater Res*. 2005;20(11):2902-2909. <https://doi.org/10.1557/jmr.2005.0382>
  45. McParland P, Taylor D, Bell S. Myofibroblast differentiation in the connective tissues of the amnion and chorion of term human fetal membranes-implications for fetal membrane rupture and labour. *Placenta*. 2000;21(1):44-53. <https://doi.org/10.1053/plac.1999.0439>
  46. Engineer N, O'Donoghue K, Wimalasundera R, Fisk N. The effect of polyhydramnios on cervical length in twins: a controlled intervention study in complicated monochorionic pregnancies. *PLoS One*. 2008;3(12):e3834. <https://doi.org/10.1371/journal.pone.0003834>
  47. Jonsson M. Induction of twin pregnancy and the risk of caesarean delivery: a cohort study. *BMC Pregnancy Childbirth*. 2015;15(1):136. <https://doi.org/10.1186/s12884-015-0566-4>
  48. Bacelis J, Juodakis J, Adams Waldorf K, et al. Uterine distention as a factor in birth timing: retrospective nationwide cohort study in Sweden. *BMJ Open*. 2018;8(10):e022929. <https://doi.org/10.1136/bmjopen-2018-022929>
  49. Norman M, Ekman G, Malmström A. Prostaglandin E2-induced ripening of the human cervix involves changes in proteoglycan metabolism. *Obstet Gynecol*. 1993;82(6):1013-1020.
  50. Norman M, Ekman G, Malmström A. Changed proteoglycan metabolism in human cervix immediately after spontaneous vaginal delivery. *Obstet Gynecol*. 1993;81(2):217-223.
  51. Park J, Romero R, Lee J, Chaemsaitong P, Chaiyasit N, Yoon BH. An elevated amniotic fluid prostaglandin F2 $\alpha$  concentration is associated with intra-amniotic inflammation/infection, and clinical and histologic chorioamnionitis, as well as impending preterm delivery in patients with preterm labor and intact membranes. *J Matern Fetal Neonatal Med*. 2015;29:1-10. <https://doi.org/10.3109/14767058.2015.1094794>
  52. Romero R, Chaiworapongsa T, Espinoza J, et al. Fetal plasma MMP-9 concentrations are elevated in preterm premature rupture of the membranes. *Am J Obstet Gynecol*. 2022;187(5):1125-1130. <https://doi.org/10.1067/mob.2002.127312>
  53. Hinz B, Gabbiani G. Mechanisms of force generation and transmission by myofibroblasts. *Curr Opin Biotechnol*. 2003;14(5):538-546. <https://doi.org/10.1016/j.copbio.2003.08.006>
  54. Tomasek J, Gabbiani G, Hinz B, Chaponnier C, Brown R. Myofibroblasts and mechano-regulation of connective tissue remodelling. *Nat Rev Mol Cell Biol*. 2002;3(5):349-363. <https://doi.org/10.1038/nrm809>
  55. Barrientos S, Stojadinovic O, Golinko MS, Brem H, Tomic-Canic M. Growth factors and cytokines in wound healing. *Wound Repair Regen*. 2008;16(5):585-601. <https://doi.org/10.1111/j.1524-475x.2008.00410.x>
  56. Wang JHC, Li B. Fibroblasts and myofibroblasts in wound healing: force generation and measurement. *J Tissue Viability*. 2011;20(20):108-120. <https://doi.org/10.1016/j.jtv.2009.11.004>
  57. Famos F, Avilla-Royo E, Vonzun L, Ochsenbein-Kolble N, Ehrbar M. Miniaturized bioengineering models for preterm fetal membrane healing. *Fetal Diagn Ther*. 2022;49(5-6):235-244. <https://doi.org/10.1159/000525559>

**How to cite this article:** Costa E, Thrasivoulou C, Becker DL, Deprest JA, David AL, Chowdhury TT. Cx43 regulates mechanotransduction mechanisms in human preterm amniotic membrane defects. *Prenat Diagn*. 2023;43(10):1284-1295. <https://doi.org/10.1002/pd.6429>